

See discussions, stats, and author profiles for this publication at: <https://www.researchgate.net/publication/43350506>

Photoinduced Electron Transfer of Oxazine 1/TiO₂ Nanoparticles at Single Molecule Level by Using Confocal Fluorescence Microscopy

ARTICLE in LANGMUIR · JUNE 2010

Impact Factor: 4.46 · DOI: 10.1021/la904273x · Source: PubMed

CITATIONS

5

READS

35

6 AUTHORS, INCLUDING:



[Jer-Shing Huang](#)

National Tsing Hua University

52 PUBLICATIONS 1,169 CITATIONS

[SEE PROFILE](#)

Photoinduced Electron Transfer of Oxazine 1/TiO₂ Nanoparticles at Single Molecule Level by Using Confocal Fluorescence Microscopy

Yi-Ju Chen, Hsin-Yu Tzeng, Hsiu-Fang Fan, Ming-Shiang Chen, Jer-Shing Huang, and King-Chuen Lin*

Department of Chemistry, National Taiwan University, Taipei 106, and Institute of Atomic and Molecular Sciences, Academia Sinica, Taipei 106, Taiwan

Received November 11, 2009. Revised Manuscript Received April 12, 2010

Kinetics of photoinduced electron transfer (ET) from oxazine 1 dye to TiO₂ nanoparticles (NPs) surface is studied at a single molecule level by using confocal fluorescence microscopy. Upon irradiation with a pulsed laser at 630 nm, the fluorescence lifetimes sampled among 100 different dye molecules are determined to yield an average lifetime of 2.9 ± 0.3 ns, which is close to the value of 3.0 ± 0.6 ns measured on the bare coverslip. The lifetime proximity suggests that most interfacial electron transfer (IFET) processes for the current system are inefficient, probably caused by physisorption between dye and the TiO₂ film. However, there might exist some molecules which are quenched before fluorescing and fail to be detected. With the aid of autocorrelation analysis under a three-level energy system, the IFET kinetics of single dye molecules in the conduction band of TiO₂ NPs is evaluated to be $(1.0 \pm 0.1) \times 10^4 \text{ s}^{-1}$ averaged over 100 single molecules and the back ET rate constant is $4.7 \pm 0.9 \text{ s}^{-1}$. When a thicker TiO₂ film is substituted, the resultant kinetic data do not make a significant difference. The trend of IFET efficacy agrees with the method of fluorescence lifetime measurements. The obtained forward ET rate constants are about ten times smaller than the photovoltage response measured in an assembled dye-sensitized solar cell. The discrepancy is discussed. The inhomogeneous and fluctuation characters for the IFET process are attributed to microenvironment variation for each single molecule. The obtained ET rates are much slower than the fluorescence relaxation. Such a small ET quantum yield is yet feasibly detectable at a single molecule level.

I. Introduction

Organic dyes blended with TiO₂ nanoparticles (NPs) have been recognized as important light harvesting materials especially in the visible spectral range.^{1–6} Efficient photoinduced electron transfer from dye molecules to nanocrystalline TiO₂ thin film is of critical importance in dye-sensitized solar cell (DSSC) design.^{7–12} The electron transfer (ET) kinetics in most dye-sensitized TiO₂ systems is as rapid as in the time regime of femtosecond to several hundred picoseconds. The injected electrons are localized in either sub-band or surface states of TiO₂ semiconductor. A fraction of the electrons, de-trapped thermally from the reduced semiconductor, possibly undergo recombination with the oxidized dye molecules. Such a back ET process takes place slowly from subnanoseconds to several milliseconds. An efficient solar cell design must prolong the lifetimes of charge-separated states by lowering the back ET rates. Therefore,

characterizing the kinetics of forward and backward ET may be conducive to facilitating the working efficiency of a solar cell design.

Thus far, fundamental characterization of the dye/TiO₂-based solar cells is usually performed on ensembles of molecules.^{1,2} The bulk measurements yield ensemble-averaged information and could mask or overlook specific phenomena occurring at the dye–semiconductor interfaces. To supplement information that might be lacking in the ensemble measurements, this work is aimed at understanding the dynamics of interfacial electron transfer (IFET) of dye molecules adsorbed on the TiO₂ NPs surface at a single molecule level. The importance of IFET phenomena has been extended to other applications of photocatalysis^{13–17} and molecular devices.^{18–20}

Analyzing fluorescence intermittency of single molecule spectroscopy (SMS) has emerged as an important method for understanding the dynamic processes of excited state molecules,^{21–25}

*To whom correspondence should be sent. Fax: 886-2-23621483 E-mail: kcln@ccms.ntu.edu.tw.

- (1) Hagfeldt, A.; Grätzel, M. *Acc. Chem. Res.* **2000**, *33*, 269–277.
- (2) Grätzel, M. *Nature* **2001**, *414*, 338–344.
- (3) Hara, K.; Horiuchi, H.; Katoh, R.; Singh, L. P.; Sugihara, H.; Sayama, K.; Murata, S.; Tachiya, M.; Arakawa, H. *J. Phys. Chem. B* **2002**, *106*, 374–379.
- (4) Cahen, D.; Hodas, G.; Grätzel, M.; Guillemoles, J. F.; Riess, I. *J. Phys. Chem. B* **2000**, *104*, 2053–2059.
- (5) Ferrere, S.; Gregg, B. A. *J. Phys. Chem. B* **2001**, *105*, 7602–7605.
- (6) Bisquert, J.; Zaban, A.; Salvador, P. *J. Phys. Chem. B* **2002**, *106*, 8774–8782.
- (7) Biju, V.; Micic, M.; Hu, D. H.; Lu, H. P. *J. Am. Chem. Soc.* **2004**, *126*, 9374–9381.
- (8) Li, B.; Zhao, J.; Onda, K.; Jordan, K. D.; Yang, J. L.; Petek, H. *Science* **2006**, *311*, 1436–1440.
- (9) Kondov, I.; Čížek, M.; Benesch, C.; Wang, H. B.; Thoss, M. *J. Phys. Chem. C* **2007**, *111*, 11970–11981.
- (10) Peter, L. M. *J. Phys. Chem. C* **2007**, *111*, 6601–6612.
- (11) Lee, J. K.; Ma, W. L.; Brabec, C. J.; Yuen, J.; Moon, J. S.; Kim, J. Y.; Lee, K.; Bazan, G. C.; Heeger, A. J. *J. Am. Chem. Soc.* **2008**, *130*, 3619–3623.
- (12) Tachikawa, T.; Cui, S. C.; Tojo, S.; Fujitsuka, M.; Majima, T. *Chem. Phys. Lett.* **2007**, *443*, 313–318.

- (13) Fox, M. A.; Dulay, M. T. *Chem. Rev.* **1993**, *93*, 341–357.
- (14) Kamat, P. V. *J. Phys. Chem. C* **2007**, *111*, 2834–2860.
- (15) Hoffmann, M. R.; Martin, S. T.; Choi, W. Y.; Bahnmann, D. W. *Chem. Rev.* **1995**, *95*, 69–96.
- (16) Naito, K.; Tachikawa, T.; Fujitsuka, M.; Majima, T. *J. Am. Chem. Soc.* **2009**, *131*, 934–936.
- (17) Tachikawa, T.; Majima, T. *Langmuir* **2009**, *25*, 7791–7802.
- (18) Mikaelian, G.; Ogawa, N.; Tu, X. W.; Ho, W. *J. Chem. Phys.* **2006**, *124*, 131101–1–131101–4.
- (19) Venkataraman, L.; Klare, J. E.; Nuckolls, C.; Hybertsen, M. S.; Steigerwald, M. L. *Nature* **2006**, *442*, 904–907.
- (20) Wang, L.; Liu, L.; Chen, W.; Feng, Y. P.; Wee, A. T. S. *J. Am. Chem. Soc.* **2006**, *128*, 8003–8007.
- (21) *Single-molecule Optical Detection, Imaging and Spectroscopy*; Basche, T., Moerner, W. E., Orrit, M., Wild, U. P., Eds; VCH: Weinheim, 1997.
- (22) Xie, X. S.; Dunn, R. C. *Science* **1994**, *265*, 361–364.
- (23) Veerman, J. A.; Garcia-Parajo, M. F.; Kuipers, L.; van Hulst, N. F. *Phys. Rev. Lett.* **1999**, *83*, 2155–2158.
- (24) Michalet, X.; Weiss, S.; Jager, M. *Chem. Rev.* **2006**, *106*, 1785–1831.
- (25) Wu, S. W.; Ogawa, N.; Ho, W. *Science* **2006**, *312*, 1362–1365.

such as triplet state behavior,^{26,27} molecular reorientation,²⁸ intersystem crossing,^{26,29–31} energy transfer,^{32–34} and spectral diffusions.^{35,36} Recently, SMS has been extended to probe photo-induced electron transfer in complicated systems including intramolecular^{34,37–43} and interfacial electron transfers.^{7,38,44–48} For instance, Adams and co-workers observed intramolecular electron transfer (IMET) in model dimer systems in which two perylene chromophores were linked via varied distance of bridge.³⁷ Although similar ET experiments have been studied in solutions, IMET appeared too slow with respect to radiative decay to be followed using bulk techniques. Cotlet et al. investigated the dynamics of photoinduced reversible electron transfer occurring between donor and acceptor in single molecules of polyphenylenic rigid dendrimer embedded in polystyrene.⁴² They found that the fluctuation of fluorescence decay times for both forward and reverse electron transfer is induced by conformation changes in the dendrimer structure and by polystyrene chain reorientation. Such detailed dynamical complexity cannot be visualized in ensemble experiments. Lu and co-workers studied photosensitized IFET processes in Coumarin 343, Cresyl Violet-TiO₂ NPs,⁷ and ZnTCPP-TiO₂ systems.⁴⁷ They found the dynamic and static IFET inhomogeneities that are characterized by the nonexponential autocorrelation function and power-law distribution of the probability density of dark times. These intermittent interfacial reaction dynamics cannot be achieved by conventional ensemble-averaged experiments.

By taking advantage of the SMS merits, the IFET phenomena of oxazine 1 dye adsorbed on the TiO₂ NPs surface is investigated in this work. We apply time-correlated single-photon counting

- (26) Yip, W.-T.; Hu, D.; Yu, J.; VandenBout, D. A.; Barbara, P. F. *J. Phys. Chem. A* **1998**, *102*, 7564–7575.
- (27) Köhn, F.; Hofkens, J.; Gronheid, R.; Van der Auweraer, M.; De Schryver, F. C. *J. Phys. Chem. A* **2002**, *106*, 4808–4814.
- (28) Ambrose, W. P.; Goodwin, P. M.; Martin, J. C.; Keller, R. A. *Phys. Rev. Lett.* **1994**, *72*, 160–163.
- (29) Bernard, J.; Fleury, L.; Talon, H.; Orrit, M. *J. Chem. Phys.* **1993**, *98*, 850–859.
- (30) van Hulst, N. F.; Veerman, J.-A.; Garcia-Parajo, M. F.; Kuipers, L. *J. Chem. Phys.* **2000**, *112*, 7799–7810.
- (31) Jia, K.; Wan, Y.; Xia, A. D.; Li, S. Y.; Gong, F. B.; Yang, G. *Q. J. Phys. Chem. A* **2007**, *111*, 1593–1597.
- (32) VandenBout, D. A.; Yip, W.-T.; Hu, D.; Fu, D.-K.; Swager, T. M.; Barbara, P. F. *Science* **1997**, *277*, 1074–1077.
- (33) Cotlet, M.; Vosch, T.; Habuchi, S.; Weil, T.; Mullen, K.; Hofkens, J.; De Schryver, F. *J. Am. Chem. Soc.* **2005**, *127*, 9760–9768.
- (34) Flors, C.; Oesterling, J.; Schnitzler, T.; Fron, E.; Schweitzer, G.; Sliwa, M.; Herrmann, A.; van der Auweraer, M.; de Schryver, F. C.; Mullen, K.; Hofkens, J. *J. Phys. Chem. C* **2007**, *111*, 4861–4870.
- (35) Xie, X. S.; Dunn, R. C. *Science* **1994**, *265*, 361–364.
- (36) Kulzer, F.; Kummer, S.; Matzke, R.; Brauchle, C.; Basche, T. *Nature* **1997**, *387*, 686–688.
- (37) Liu, R.; Holman, M. W.; Zang, L.; Adams, D. M. *J. Phys. Chem. A* **2003**, *107*, 6522–6526.
- (38) Holman, M. W.; Adams, D. M. *ChemPhysChem* **2004**, *5*, 1831–1836.
- (39) Bell, T. D. M.; Stefan, A.; Masuo, S.; Vosch, T.; Lor, M.; Cotlet, M.; Hofkens, J.; Bernhardt, S.; Mullen, K.; van der Auweraer, M.; Verhoeven, J. W.; De Schryver, F. C. *ChemPhysChem* **2005**, *6*, 942–948.
- (40) Cotlet, M.; Masuo, S.; Lor, M.; Fron, E.; van der Auweraer, M.; Mullen, K.; Hofkens, J.; De Schryver, F. C. *Angew. Chem., Int. Ed.* **2004**, *43*, 6113–6116.
- (41) Holman, M. W.; Liu, R. C.; Zang, L.; Yan, P.; DiBenedetto, S. A.; Bowers, R. D.; Adams, D. M. *J. Am. Chem. Soc.* **2004**, *126*, 16126–16133.
- (42) Cotlet, M.; Masuo, S.; Luo, G.; Hofkens, J.; Van der Auweraer, M.; Verhoeven, J.; Mullen, K.; Xie, X. S.; De Schryver, F. *Proc. Natl. Acad. Sci. U.S.A.* **2004**, *101*, 14343–14348.
- (43) Siekierzycka, J. R.; Hippius, C.; Würthner, F.; Williams, R. M.; Brouwer, A. M. *J. Am. Chem. Soc.* **2010**, *132*, 1240–1242.
- (44) Lu, H. P.; Xie, X. S. *J. Phys. Chem. B* **1997**, *101*, 2753–2757.
- (45) Bell, T. D. M.; Pagba, C.; Myahkostupov, M.; Hofkens, J.; Piotrowiak, P. *J. Phys. Chem. B* **2006**, *110*, 25314–25321.
- (46) Natelson, D.; Yu, L. H.; Ciszek, J. W.; Keane, Z. K.; Tour, J. M. *Chem. Phys.* **2006**, *324*, 267–275.
- (47) Yuanmin, W.; Xuefei, W.; Sujit, K. G.; Lu, H. P. *J. Am. Chem. Soc.* **2009**, *131*, 1479–1487.
- (48) Holman, M. W.; Liu, R. C.; Adams, D. M. *J. Am. Chem. Soc.* **2003**, *125*, 12649–12654.

(TCSPC) to measure fluorescence lifetimes among 100 individual molecules. Comparison of the average lifetime with that determined on a bare coverslip reveals that most IFET processes in the current system are slow and inefficient. For obtaining quantitative kinetic data, we acquire single-molecule fluorescence trajectories, characteristic of “on” and “off” blinking with time, in which the intensity fluctuation is considered to be mainly attributed to the IFET behavior. The fluorescent dye molecule lies in an off-blinking state when its electron moves to the TiO₂ NPs conduction band. While the electron transfers back to the oxidized state, the dye molecule blinks “on” again following photoexcitation. In this work, the autocorrelation function is used to analyze discrete fluorescence intensity jumps between “on” and “off” levels. The “on” and “off” lifetimes and the subsequent rate constants of forward and backward electron transfers are then determined. Finally, the ET kinetics at a single molecule level is compared to photovoltage response measured in an assembled DSSC.

II. Experimental Section

A. Apparatus. All single molecule experiments were performed with a confocal fluorescence microscope (DM IRM, Leica). A single-mode pulsed laser at 630 nm, with a repetition rate of 10 MHz and pulsed duration of 280 ps, was used as the excitation source (PDL800, PicoQuant, GmbH). The beam collimated with a pair of lenses was spectrally filtered with an excitation filter (Z630/10×, Chroma) before entering an inverted microscope. An oil immersion objective (100×, NA1.25, Nikon) was used both to focus the laser beam onto the sample, prepared on the surface of a silica coverslip, and to collect fluorescence from the sample. The excitation intensity of the pulsed beam was constantly measured to be $38.5 \pm 1.2 \text{ W/cm}^2$ right on the top of the bare coverslip throughout the experiments. The fluorescence, after transmitting through a dichroic mirror (Z630RDC, Chroma), was refocused by a tube lens (200 mm focal length) onto an optical fiber (62.5 μm diameter) which was coupled to an avalanche photodiode (APD) detector with a 175 μm active area (SPAD, AQR-14, Perkin-Elmer). Here, the fiber serves as a pinhole to reject out-of-focus light. The fluorescence signal may also be reflected simultaneously to a charge-coupled device (CCD) (Andor DV 412) by a beamsplitter. A notch filter (CVI, RNF 630 nm, 6 < OD) and a bandpass filter (HQ667/30 m) were positioned in front of the detector to remove excitation background. A simple method to record wide-field fluorescence images with a CCD detector was by inserting a 30 cm focal length lens before the collimated beam entered the microscope. Then, the single molecule that fluoresced was readily moved to a particular position to be illuminated using a *x*-*y* positioning stage. The fluorescence lifetime of a single molecule was measured by time-correlated single-photon counting (TCSPC) with a TimeHarp 200 PCI-board (PicoQuant). The data were stored in a time-tagged time-resolved mode, which allowed recording every detected photon and its individual timing information. The TCSPC curve was analyzed by single exponential tail-fit taking into account deconvolution of the instrument response time (SymPhoTime by PicoQuant). The data collection spread from 2080 to 3456 channels, while data analysis was usually narrowed to the 2850–3300 channel slot. Up to 1000 photon counts prior to photobleaching are used for the lifetime measurement.

B. Material Preparation. The TiO₂ precursor was prepared by a sol–gel process. 72 mL of 98% titanium(IV) isopropoxide (Across) was added to 430 mL of 0.1 M nitric acid solution, which was then stirred and heated to 85 °C for 8 h. The colloid, as filtered from the cooled mixture, was heated again in an autoclave at five temperatures of 180, 200, 220, 240, and 260 °C for 12 h to grow TiO₂ NPs. The TiO₂ colloid was concentrated to 13 wt %, followed by addition of a 30 wt % (with respect to TiO₂) of poly(ethylene glycol) (Merck) to prevent cracking during drying.

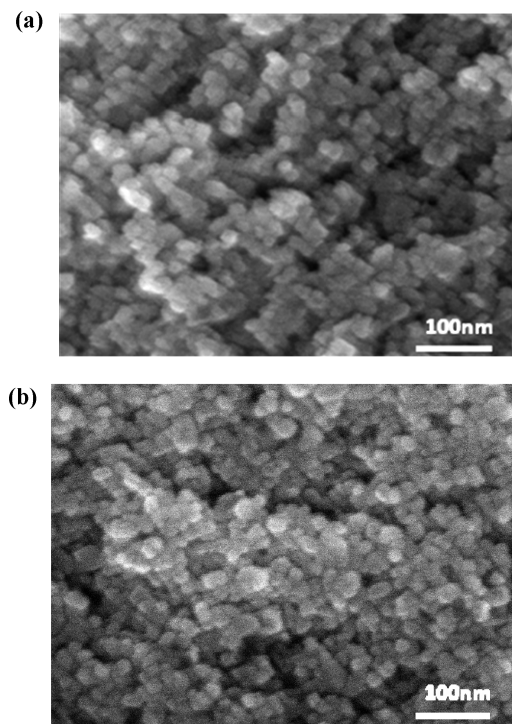


Figure 1. Images of TiO_2 NP film using scanning electron microscopy: (a) thin film fabricated by spin-coating, (b) thick film by glass rod method. The average sizes of TiO_2 NPs are about 20 nm for both films.

For single molecule experiments, two types of TiO_2 NPs films were fabricated with different thicknesses. The thin film was made by spin-coating, while the thick film of $< 6 \mu\text{m}$ was made by spreading TiO_2 colloid on a coverslip with a glass rod. To prepare for the thin film, a $40 \mu\text{L}$ aliquot of 0.65% TiO_2 NPs was spin-coated on a cleaned coverslip. The same process was repeated four times to ensure TiO_2 coated the coverslip well. For making the thick film, TiO_2 colloid (13 wt %) was spread directly on the coverslip by a glass rod. After drying in the air for 30 min, both thin and thick films were heated to 450°C at a rate of $20^\circ\text{C}/\text{min}$ and remained for 30 min before cooling to the room temperature. The phase and the size of TiO_2 NPs were characterized by using scanning electron microscopy. As shown in Figure 1a,b, the thin and thick films were well-covered over the coverslip to ensure that the oxazine 1 dye may be fully adsorbed on the TiO_2 NP-coated surfaces. The enlarged images displayed the TiO_2 NPs size of $\sim 20 nm for both films. A $30 \mu\text{L}$ drop of 0.1 nM oxazine 1 dye in methanol solution was spin-coated over the TiO_2 NPs surface, and then put on the sample stage of the microscope for fluorescence measurement.$

For the photovoltaic experiments, the TiO_2 paste was spread on a fluorine-doped tin oxide (FTO) conducting glass by a glass rod.⁴⁹ The TiO_2 film electrode, after heating to 80°C , was then immersed in a $3 \times 10^{-4} \text{ M}$ of oxazine 1 dye aqueous solution for 12 h. A FTO glass platinized with about $0.1\text{-}\mu\text{m}$ -thick Pt by sputtering was used as a counter electrode. Both electrodes were clipped with a hot-melt sheet (Surlyn 1702, DuPont) and heated at 80°C on a hot plate. The electrolyte, which comprised a mixture of 0.5 M LiI, 0.05 M I_2 , and 0.5 M 4-*tert*-butylpyridine in acetonitrile, was injected into the cell through either one of the open holes. Then, the cell was sealed with a Torr Seal sealant. For the photovoltaic measurements, the assembled DSSC was irradiated with a 5–8 ns pulsed dye laser (PDL-2, Spectra-Physics) at 630 nm , which was pumped by a second harmonic of Nd:YAG laser (PRO-190, Spectra-Physics)

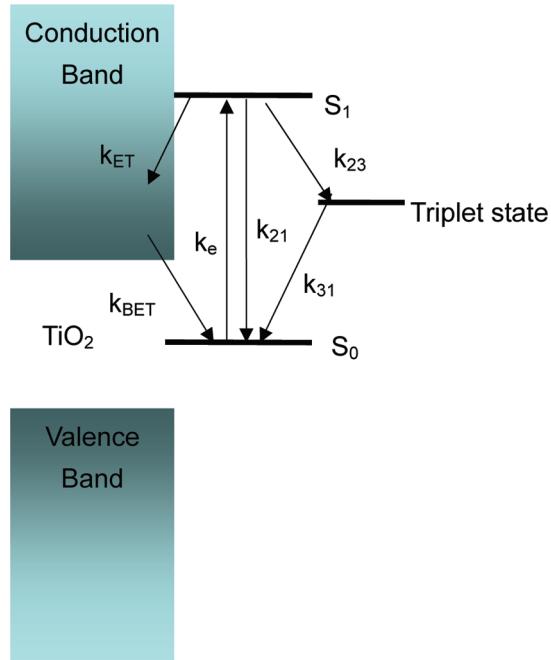


Figure 2. Schematic energy diagram for a dye-sensitized TiO_2 system. Four levels are involved, singlet ground and excited states, triplet state populated via intersystem crossing, and TiO_2 conduction band in which interfacial electron transfer occurs. The related rate constants are indicated.

operating at 10 Hz. The light was guided to irradiate the TiO_2 film serving as photoanode where spectral absorption by the oxazine 1 molecules occurred. Following photoinduced molecular electron injection through the outside circuit, the photovoltage response was recorded with a transient digitizer (LT322, LeCroy).

III. Theoretical Background

As shown in Figure 2, when the oxazine 1 molecules are adsorbed on the TiO_2 NPs surface, a four-level energy scheme is formed including singlet ground, singlet excited, and triplet states of the dye molecule, as well as a conduction band. Upon irradiation with a laser source, the population in the excited state may undergo various deactivation processes. The related transitions are displayed in Figure 2. Because the selected dye molecule has a relatively short triplet excursion, the fluorescence in the absence of TiO_2 film becomes a constant average intensity with near shot-noise-limited fluctuation.^{38,50} As a result, the system can be simplified to a three-level energy scheme.

As the ET process occurs, the fluorescence appears to blink on and off. The transition between the on and off states may be considered as feeding between the singlet and the conduction subspaces²⁶



The on-state rate constant is equivalent to the backward ET rate constant from the conduction band, i.e.,

$$k_{\text{on}} = k_{\text{bet}} \quad (2)$$

(50) Haase, M.; Hubner, C. G.; Reuther, E.; Herrmann, A.; Mullen, K.; Basche, Th. *J. Phys. Chem. B* **2004**, *108*, 10445–10450.

while the off-state rate constant corresponds to the excitation rate constant k_{ex} multiplied by the fraction of population relaxing to the conduction band, as expressed by

$$k_{\text{off}} = \frac{k_{\text{et}}}{k_{21} + k_{\text{et}}} k_{\text{ex}} \quad (3)$$

Here, k_{21} is the relaxation rate constant from the state 2 to 1 containing the radiative and nonradiative processes, and k_{et} is the forward ET rate constant. k_{ex} is related to the excitation intensity I_o (units of erg/cm² s) by

$$k_{\text{ex}} = \sigma I_o / h\nu \quad (4)$$

where σ is the absorption cross section and $h\nu$ is the photon energy. The average residence times in the on and off states correspond to the reciprocal of the feeding rate in the off and on states, respectively. That is, $\tau_{\text{on}} = 1/k_{\text{off}}$ and $\tau_{\text{off}} = 1/k_{\text{on}}$.

When the blinking behavior is not well-resolved, the rate constants in on–off transition may be quantified by analyzing autocorrelation of fluorescence intensities.³⁸ The normalized autocorrelation function is defined as the rate of detecting pairs of photons separated in time by an interval τ , relative to the rate when the photons are uncorrelated. It is expressed as

$$G(\tau) = \frac{\langle I(t)I(t+\tau) \rangle}{\langle I(t) \rangle^2} \quad (5)$$

where $I(t)$ is the fluorescence intensity at time t and τ is the correlation time. The bracketed term denotes the intensity average over time. When the population relaxation is dominated by the singlet decay, the autocorrelation function may be simplified to an exponential decay, i.e.,

$$G(\tau) = A + B e^{-k\tau} \quad (6)$$

where A is an offset constant, B a pre-exponential factor, and k the decay rate constant. They are determined by fitting to the autocorrelation data. These parameters are explicitly related to the phenomena of on/off blinking due to the ET processes by

$$k = k_{\text{on}} + k_{\text{off}} \quad (7)$$

and

$$\frac{B}{A} = \frac{k_{\text{on}} k_{\text{off}} (I_{\text{on}} - I_{\text{off}})}{(k_{\text{on}} I_{\text{on}} + k_{\text{off}} I_{\text{off}})^2} \quad (8)$$

If $I_{\text{on}} \gg I_{\text{off}}$, then the above equation is simplified to

$$\frac{B}{A} = \frac{k_{\text{off}}}{k_{\text{on}}} \quad (9)$$

The forward and backward ET rate constants in the dye molecule-TiO₂ NPs system can thus be evaluated.

IV. Results and Discussion

A. Fluorescence Lifetimes. Figure 3 shows absorption spectra of oxazine 1 solution in the presence (or absence) of TiO₂ NPs by means of ensemble measurements. The absorption cross section reaches as large as $\sim 3.5 \times 10^{-16}$ cm² at 630 nm. The fluorescence

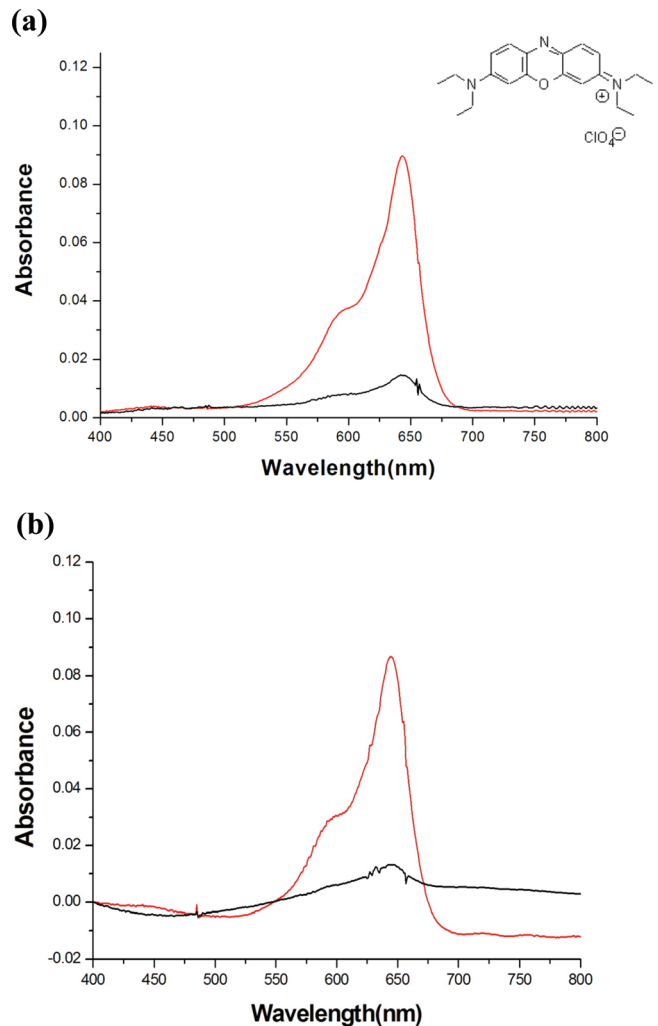


Figure 3. (a) Absorption spectra of oxazine 1 dye in methanol solution with concentration of 1×10^{-6} (larger peak) and 1×10^{-8} M, respectively. Oxazine 1 structure is also displayed. (b) Absorption spectra of oxazine 1 methanol solution with concentration of 1×10^{-6} (larger peak) and 1×10^{-8} M, respectively, in the presence of TiO₂ NPs.

quantum yield is 0.11 in ethanol as the solvent and increases to 0.19 in ethylene glycol.⁵¹ When the dye in methanol solution is diluted from 10^{-6} to 10^{-8} M, the spectral profile remains the same with a major peak and a minor shoulder. The spectra appear almost the same between the conditions with and without TiO₂ NP involvement. The results suggest that the dimer contribution should be minor and negligible. Otherwise, the small shoulder will grow gradually to be comparable with the other major peak.

A 10^{-10} M of oxazine 1 dye solution was spin-coated on a bare or TiO₂ NP-coated coverslip. Figure 4a displays the fluorescence images of the single oxazine 1 molecules within a $24 \mu\text{m} \times 24 \mu\text{m}$ area on the bare coverslip, as excited by a pulsed laser at 630 nm with excitation intensity of $39 \pm 2 \text{ W/cm}^2$. Each bright spot is attributed to a single molecular fluorescence. The spot size of about $\sim 650 \text{ nm}$ is restricted by the diffraction limit. Figure 4b shows the background emissions of the TiO₂ NPs surface. Stray light scattered by the TiO₂ NPs causes background noise, which is somehow dimmer than those fluorescent spots from the dye molecules. Figure 4c shows the single molecular fluorescence images of dye molecules adsorbed on the TiO₂ NP surface. The maximum fluorescence intensity reaches 650 counts acquired by a CCD within an integration time of 0.5 s. It is found that the

(51) Sens, R.; Drexhage, K. H. *J. Luminesc.* **1981**, *24*, 709–712.

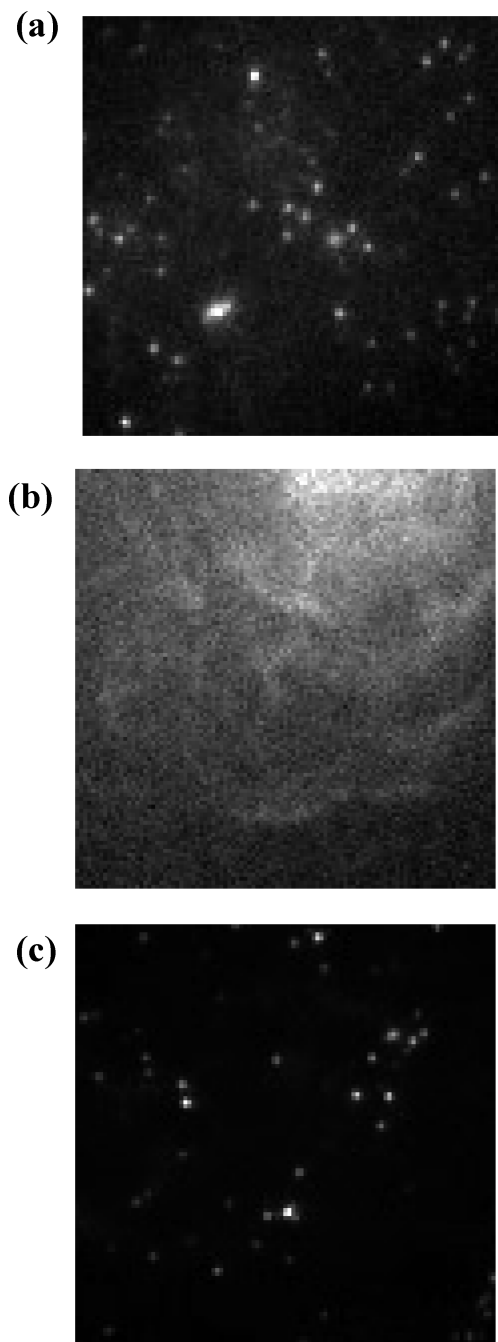


Figure 4. Fluorescence images of (a) oxazine 1 molecules on bare coverslip, (b) TiO₂ NP film without dye molecules involved, and (c) oxazine 1 molecules on TiO₂ NPs-coated coverslip.

fluorescent spots have different intensities, which may result from variation of molecular orientation and microenvironments. While counting the surface density of oxazine 1 that fluoresces on either bare or TiO₂ NPs-coated coverslip, a value of 0.088 or 0.085 per μm^2 is obtained, respectively, with an uncertainty of $\pm 10\%$. It is difficult to make a comparison with the surface density prepared initially, since a great amount of dye solution is sputtered away during the spin-coating process. Note that the roughness of the TiO₂ NPs-coated coverslip may reduce the dye molecules from sputtering away to some extents, as compared to a smooth bare glass. Although the surface density of fluorescent spots is similar among them, some molecules in the excitation might be quenched by a faster IFET process before fluorescing and thus fail to be detected. The clefts or interstices in the TiO₂ film are probably ideal sites for effective IFET.

As shown in Figure 5a, fluorescence decay of a single dye molecule on the TiO₂ NPs thin film is obtained for the lifetime measurements by time-correlated single-photon counting. The decay curve is fitted to a single exponential function, yielding a lifetime of 2.6 ns. Convolution of laser duration and instrument response is evaluated at about 550 ps, which is also shown in the figure. In this manner, the lifetimes successively determined among 100 different oxazine 1 molecules are distributed in Figure 5b, with an average value of 2.9 ± 0.3 ns. The lifetime scattering reveals an inhomogeneous character among the dye molecules measured, because of variation of dipole orientation, transition frequency, and molecular polarization on the surface. In addition, the fluctuation of the lifetime is partially attributed to the power density variation which is about $\pm 3\%$. The obtained fluorescence lifetimes are longer by 0.7 to 1.5 ns than those measured in solution.⁵² A decreased flexibility of the molecules adsorbed on the semiconductor slightly prolongs the excited state lifetimes. For comparison, the lifetimes of oxazine 1 molecules on the bare coverslip are measured analogously, and the average lifetime over 100 different molecules is 3.0 ± 0.6 ns.

The fluorescence lifetime determination of a single molecule has been demonstrated as an efficient measure of the interfacial electron transfer.^{7,38,44} In a similar experiment reported earlier, Lu and Xie observed the fluorescence lifetimes as short as 100–700 ps for single cresyl violet molecules on indium tin oxide (ITO)-coated coverslip, as compared with the radiative lifetime of 2.5–3 ns for the single dye molecules on a bare coverslip.⁴⁴ The fast decay was attributed to the IFET process, of which the rate constant may be evaluated by comparison of the two lifetimes.

In our case, despite no statistical difference with the uncertainty considered, the average lifetime of the dye on the TiO₂ film is significantly smaller than that on the bare coverslip. While inspecting Figure 5b, the asymmetric distribution shows more molecules lying on the side of shorter fluorescence lifetime. It suggests two points. First, some molecules might undergo an even faster IFET process such that the excited-state lifetimes become too short to be detected. Second, the slight difference of the fluorescence lifetimes implies that most IFET processes should be slow and inefficient. The oxazine 1 molecule lacks effective anchoring groups like carboxylate in metal–polypyridine complexes to covalently bind the dye to the semiconductor.^{53,54} These dye molecules randomly selected are anticipated to be physisorbed to the TiO₂ NPs surface or loosely trapped at the NPs interstices. Even with an efficient dye sensitizer, the preparation procedure of dye–semiconductor system affects the efficacy of electron transfer. For instance, by using TCSPC microscopy, Bell et al. observed multiexponential fluorescence decay with some components as long as 220 ns for Ru(bpy)₂(dcbpy)²⁺ dye-sensitized mesoporous films of TiO₂.⁴⁵ In contrast, the lifetimes were dramatically shortened to a subnanosecond after several times of dialysis of the dye-sensitized particles prior to deposition on the glass substrate. Since the physisorbed and trapped dye molecules should have been removed by the repeated dialysis, the residual emission stems from those covalently bound to the TiO₂ surface. However, that does not mean all interactions based on physisorption cannot lead to efficient electron transfer. Some organic dyes such as cyanine or xanthene dyes incorporated in Langmuir–Blodgett films deposited on In₂O₃ or SnO₂ electrodes show very efficient electron transfer even without chemisorptions, due to a large

(52) Landgraf, S.; Grampf, G. *Monatsh. Chem.* **2000**, *131*, 839–848.

(53) O'Regan, B.; Grätzel, M. *Nature (London)* **1991**, *353*, 737–740.

(54) Ramakrishna, G.; Jose, D. A.; Kumar, D. K.; Gas, A.; Palit, D. K.; Ghosh, H. N. *J. Phys. Chem. B* **2005**, *109*, 15445–15453.

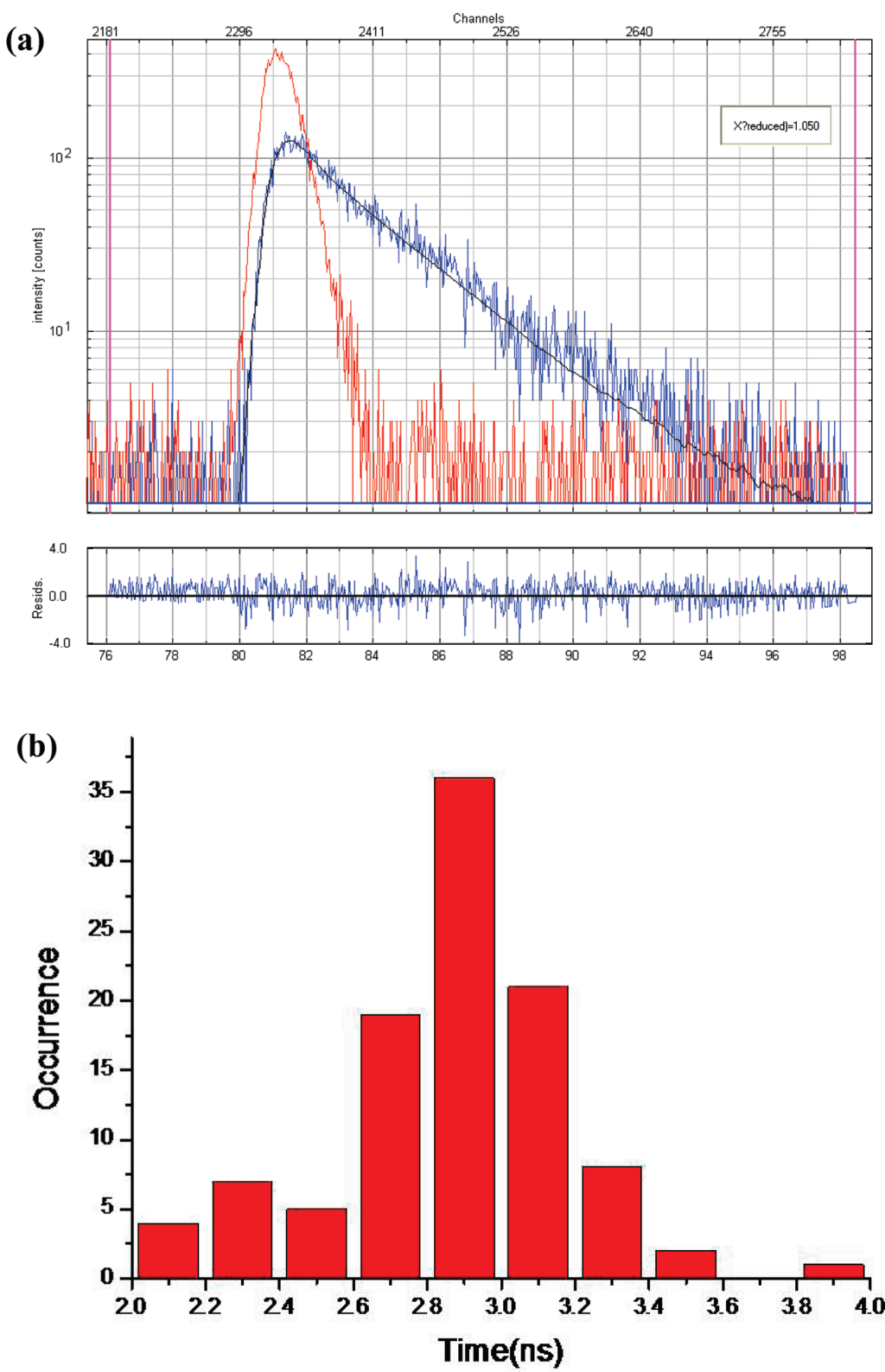


Figure 5. (a) Fluorescence decay of single oxazine 1 molecule in the presence of TiO_2 NPs measured by using time-correlated single photon counting. The instrument response function gives a faster decay estimated to be 550 ps. (b) Distribution of excited state lifetimes among 100 single oxazine 1 molecules on the TiO_2 NPs surface, yielding an average lifetime of about 2.86 ns.

free-energy difference between the LUMO of the dye and the edge of the conduction band of the semiconductor.^{55–57}

B. Fluorescence Intensity Trajectories. Now that inefficient IFET processes for the current system have been realized in the excited-state lifetime measurements, quantitative kinetic data

(55) Arden, W.; Fromherz, P. *J. Electrochem. Soc.* **1980**, *127*, 370–378.

(56) Biesmans, G.; Van der Auweraer, M.; Cathry, C.; De Schryver, F. C.; Yonezawa, Y.; Sato, T. *Chem. Phys.* **1992**, *160*, 97–121.

(57) Biesmans, C.; Van der Auweraer, M.; Cathry, C.; Meerschaut, D.; De Schryver, F. C.; Storck, W.; Willig, F. *J. Phys. Chem.* **1991**, *95*, 3771–3779.

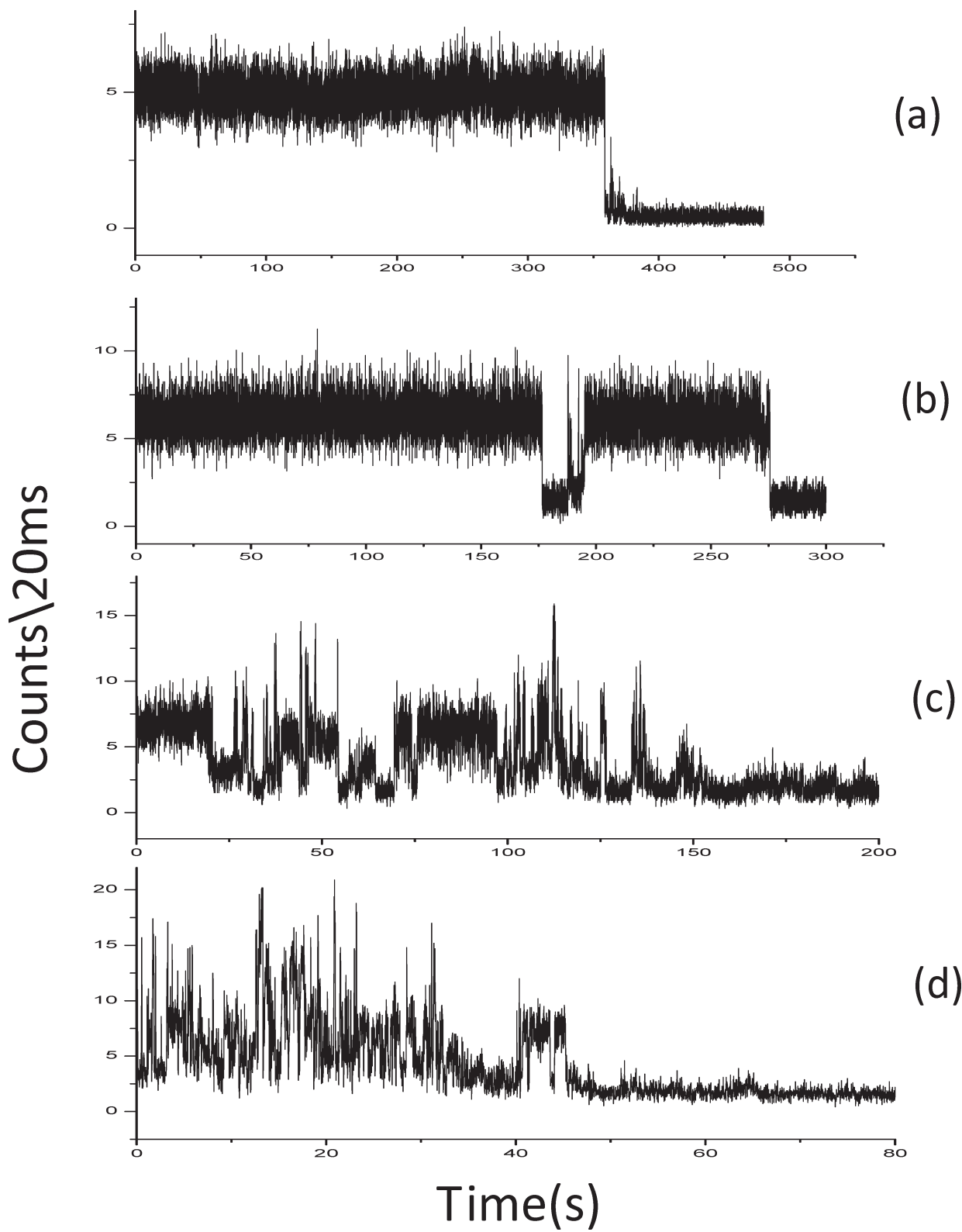


Figure 6. Fluorescence trajectories recorded for single oxazine 1 molecules (a) on bare coverslip and (b–d) on TiO₂ NPs-coated coverslip.

may be further determined by employing the following method of fluorescence trajectories. Figure 6a displays fluorescence intensity as a function of running time of a single oxazine 1 molecule on the bare coverslip with a 20 ms binning time to record the photon counts of emission. These time scales average out any faster fluorescence fluctuation or blinking of the dye molecules. The single-molecule trace shows a constant level of fluorescence

intensity which then drops to the background in one step when photobleaching occurs. Wilkinson et al. reported the triplet-state lifetime of oxazine 1 in acetonitrile solution to be 14.5 μ s,⁵⁸ and a significantly longer lifetime is yet expected for the dye adsorbed

(58) Wilkinson, F.; Kelly, G. P.; Ferreira, L. F. V.; Freire, V. M. M. R.; Ferreira, M. I. *J. Chem. Soc. Faraday Trans.* **1991**, *87*, 547–552.

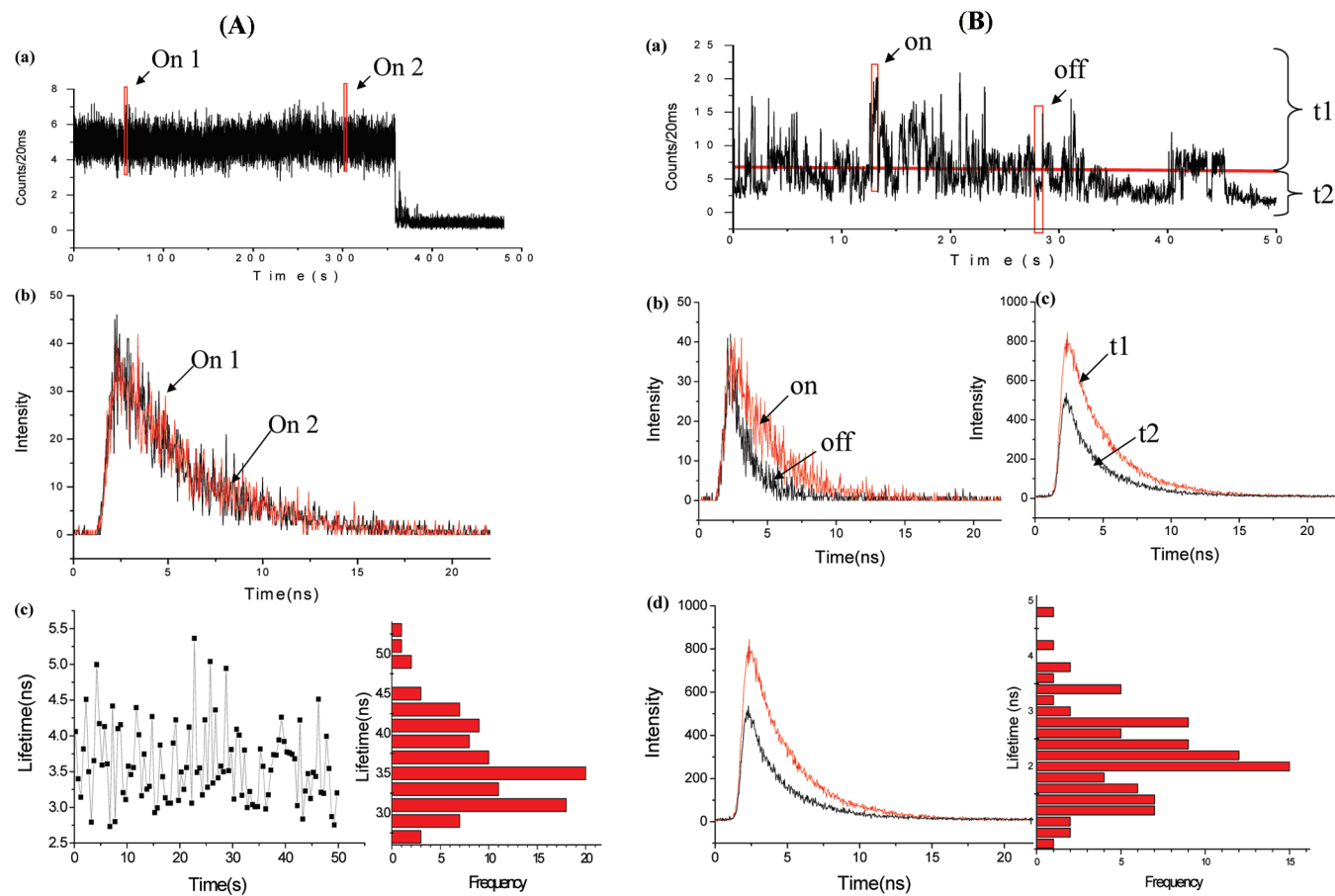


Figure 7. (A) Single-molecule fluorescence decay profile of oxazine 1 on bare glass. (a) The fluorescence intensity fluctuation slotted at 1 and 2 positions each within 1 s window. (b) Fluorescence decay profile for the 1 and 2 slots gives rise to the decay times of 3.63 and 3.59 ns, respectively. (c) The lifetime (binning window 0.5 s) fluctuation trajectory (left) and the histogram for the lifetime trajectory from 0 to 50 s before photobleaching. The average lifetime is 3.44 ± 0.48 ns. (B) Single-molecule fluorescence decay profile of oxazine 1 on TiO₂ NPs film. (a) The fluorescence intensity fluctuation slotted at one “on” position and the other “off” position. (b) Fluorescence decay profile for the “on” and “off” slots gives rise to the decay time of 2.93 and 1.26 ns, respectively. (c) Given a threshold set at 7 photocounts/20 ms, the emission trajectory is separated to a higher level and lower level. Fluorescence decay profiles for high and low intensity have similar results to the “on” and “off” slots in (b). (d) The lifetime (binning window 0.5 s) fluctuation in a range from 0.6 to 4.8 ns (left), and the histogram for the lifetime trajectory from 0 to 50 s before photobleaching.

on the solid film. A constant level of fluorescence intensity in Figure 6a implies that the prolonged lifetimes should be much shorter than the integration time adopted such that the triplet blinking may be smeared out. When 100 single molecules are sampled, about 70% display trajectories like Figure 6a. The remaining show blinks occasionally before photobleaching, in part because of photoinduced electron transfer to impurity sites of the silica coverslip. It is difficult to observe clearly triplet blinking of the single molecule caused by intersystem crossing. Instead, an average intensity of 5 counts/20 ms appears. The triplet-state lifetime if assumed to be 14.5 μ s amounts to 0.003 count, which is too weak to be resolved temporally.

As shown in Figure 7A(a), when the single-molecule fluorescence intensity trajectory of the dye molecules on the bare cover-slip is slotted within a 1 s window, the fluorescence decay lifetimes are measured to be 3.63 and 3.59 ns for the time periods of 54–55 s and 266–267 s, respectively (Figure 7A(b)). Alternatively, the lifetime fluctuation trajectory binned in a 0.5 s window gives rise to an average lifetime of 3.4 ± 0.5 ns (Figure 7A(c)), which is consistent with that averaged over 100 molecules. These facts indicate that the fluorescence intensity fluctuation for oxazine 1 on bare glass is dominated by the k_{21} rate constant, a radiative relaxation process from the singlet state. A long-shelved effect is

not observed, thus supporting the assumption that the triplet-state blinking is too weak to be resolved in our system. An autocorrelation function based on the fluorescence intensity trajectory is further analyzed. As shown in Figure 8a, the result turns out to be noisy ranging from zero to microseconds. The dynamic information of the triplet state cannot be resolved, consistent with the analyzed results of fluorescence decay times.

As shown in Figure 6b–d, the fluorescence trajectories of individual dye molecules in the presence of TiO₂ NP thin film are obtained ranging from several microseconds to seconds before photobleaching. These trajectories are classified into three types out of 100 single dye molecules as sampled. About 20% of molecules yield the traces as in Figure 6b, in which the interaction with TiO₂ NPs is weak such that the molecule fluoresces most times. A 60% majority show the traces as in Figure 6c, in which a stronger interaction is found and the “off” time becomes longer. The remaining 20% give the traces as in Figure 6d, in which the molecules stay longer at “off” time. The molecule in Figure 6d should have relatively active electron transfer such that the fluorescence process is suppressed. Figure 6d is used as an example. The fluorescence intensity trajectory is slotted within a 500 photon binned window to select one “on” intensity and the other “off” intensity (Figure 7B(a)). Analyzing the fluorescence

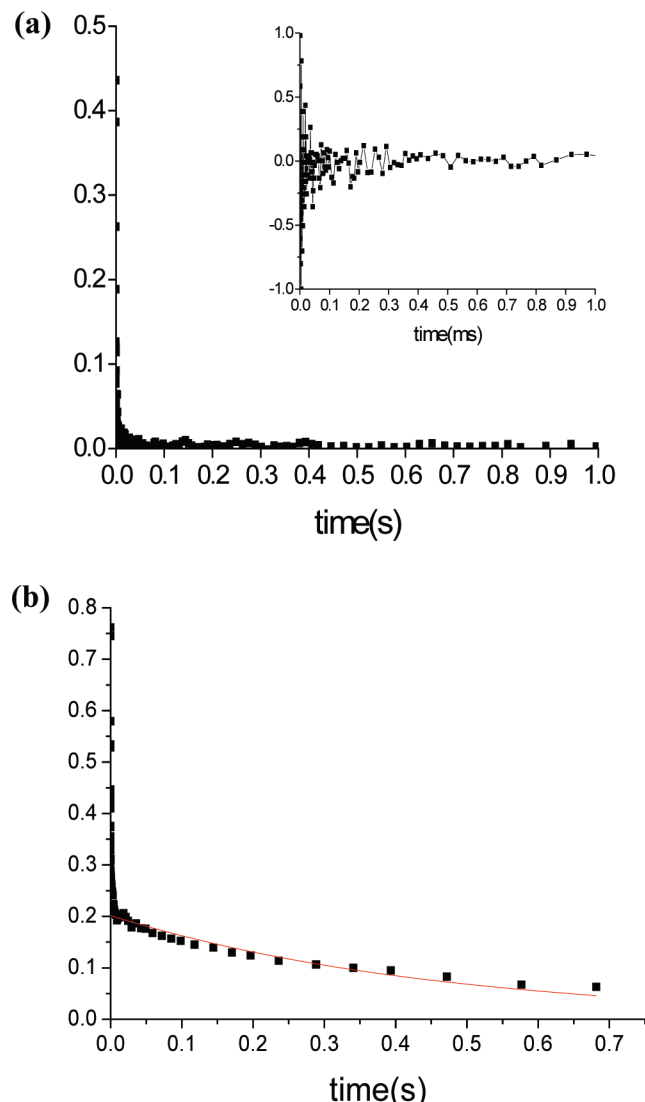


Figure 8. Autocorrelation function of fluorescence intensity from single oxazine 1 molecules (a) on bare coverslip and (b) on TiO_2 NPs-coated coverslip. The inset in (a) is the enlarged trace within the range of 1 ms.

decay yields results of 2.93 and 1.26 ns for the “on” (12.85–13.33 s slot) and “off” (29.15–30.20 s slot) lifetimes, respectively (Figure 7B(b)). Given a threshold set at 7 counts/20 ms, the fluorescence intensity is divided into a higher level and lower level. The lifetime analysis of these two levels yields results similar to those obtained in the above time slots. The “on” state shows a 2-fold longer lifetime than the “off” state (Figure 7B(c)). This fact indicates that the fluorescence intensity fluctuation is caused by both factors of reactivity and rate of electron transfer. In contrast to our case, in an analogous analysis of single-molecule fluorescence lifetime fluctuation of porphyrin on TiO_2 NPs, Lu and co-workers found that the bright and dark levels yield almost the same lifetimes except for pre-exponential factors.⁵⁹ They attributed the fluorescence intensity fluctuation to the reactivity of IFET, i.e., the fraction of IFET occurrence frequency, but not the rate of IFET which proceeds as rapidly as in the femtosecond to picosecond regime. While inspecting the fluorescence lifetime fluctuation

(59) Wang, Y.; Wang, X.; Ghosh, S. K.; Lu, H. P. *J. Am. Chem. Soc.* **2009**, *131*, 1479–1487.

Table 1. Excited-State Lifetimes and Kinetic Data for the Single-Molecule Traces Shown in Figure 6⁶

	lifetime/ns	τ_{on} (s)	τ_{off} (s)	k_{et} (s^{-1})	k_{bet} (s^{-1})
A	4.0	-	-	-	-
B	3.4	86.02	1.43	1.6×10^2	0.7
C	3.1	2.75	0.55	5.4×10^3	1.8
D	2.9	0.49	0.08	3.2×10^4	12.0

trajectory, the lifetimes analyzed within the 0.5 s window fluctuate in the range from 0.6 to 4.8 ns, which is more widely scattered than those acquired on the bare glass (Figure 7B(d)). This phenomenon suggests the existence of an additional depopulation pathway, in agreement with those of fluorescence lifetime measurements, in which slightly different lifetimes between TiO_2 film and bare coverslip are found. The additional depopulation pathway is mainly ascribed to electron transfer between oxazine 1 and TiO_2 NPs. However, other contributions such as rotational and translational motion of the dye on the TiO_2 film cannot be ruled out without information of polarization dependence of the fluorescence intensity.⁷

Since the triplet-state excursion is short, the above-mentioned equations derived for a three-level system can be validly applied to understand the interaction between the dye molecule and the TiO_2 NPs surface. Note that the contribution from triplet-state blinking is excluded. To evaluate the individual “on” and “off” times, the autocorrelation function is used to analyze the fluorescence trajectories. Figure 6c is used as an example; the autocorrelation function is fitted to a single exponential decay, yielding a B/A value of 0.2 and k of 2.17 s^{-1} . The result is shown in Figure 8b. Given the excitation rate constant k_{ex} of $2.2 \times 10^4 \text{ s}^{-1}$ (38.5 W/cm^2 was used) and the fluorescence decay k_{21} of $3.28 \times 10^8 \text{ s}^{-1}$ determined in the excited-state lifetime measurement, the IFET rate constant k_{et} , and the back ET rate constant k_{bet} are evaluated to be 5.4×10^3 and 1.8 s^{-1} , respectively, according to eqs 2, 3, 7, and 9. The IFET and back ET rate constants with the “on” and “off” times for the examples in Figure 6b–d are listed in Table 1. For comparison, the corresponding lifetime measurements are also listed. A more efficient IFET is apparently accompanied by a shorter excited-state lifetime.

As with the above examples, 100 single dye molecules are successively analyzed. The resulting IFET and back ET rate constants are displayed in the form of a histogram (Figure 9a,b), yielding ranges 10^2 – 10^4 and 0.1 – 10 s^{-1} , respectively. The distributions are fitted with an individual single-exponential function to yield an average value of $(1.0 \pm 0.1) \times 10^4$ and $4.7 \pm 0.9 \text{ s}^{-1}$, which are the upper limit of the IFET and back ET rate constants among these 100 single molecules analyzed, if the unknown contributions of rotational and translational motion are considered. The obtained average rate of electron transfer is much slower than the fluorescence relaxation. That is why no statistical difference of the fluorescence lifetimes of the dye is found between TiO_2 film and bare coverslip. However, while inspecting the average fluorescence lifetime between them, the small difference might suggest a slight increase in nonradiative relaxation processes such as internal conversion when the dye is on the TiO_2 film. The ET rate constant distribution could be affected by different orientation and distance between dye molecule and TiO_2 NPs. The weak coupling between electron donor and acceptor may be caused by physisorption between the dye molecule and the TiO_2 NPs or a disfavored energy system for the dye electron jumping into the conduction band of the semiconductor. The resulting ET quantum yield as small as 3.1×10^{-5} is difficult to detect in the ensemble system. Nevertheless, such slow electron transfer events are feasibly detectable at a single molecule level as demonstrated in this work.

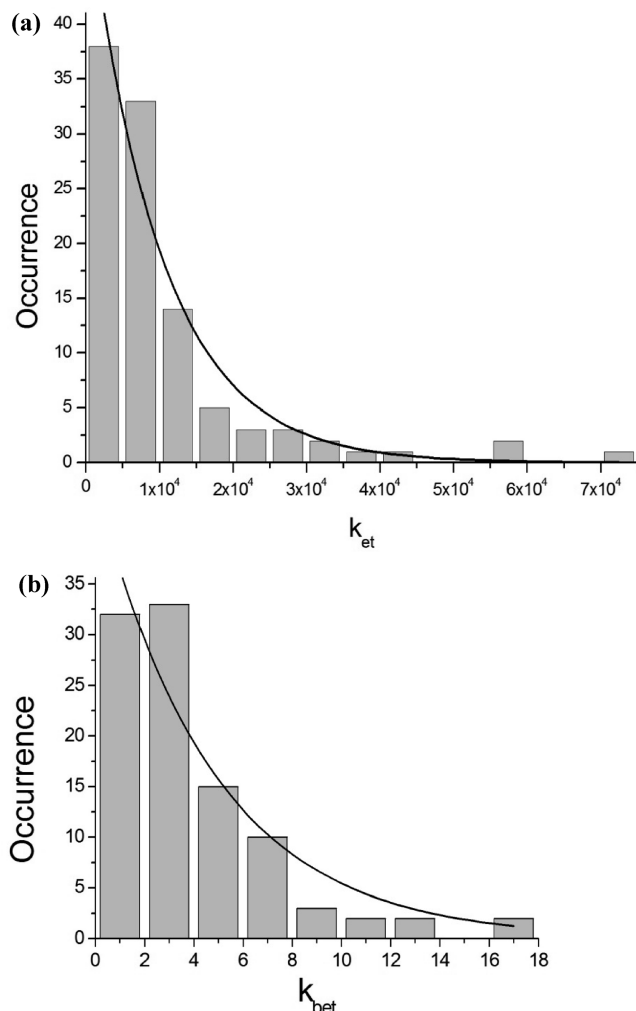


Figure 9. Histograms of (a) k_{et} and (b) k_{bet} determined among 100 dye molecules. The average values of $(1.0 \pm 0.1) \times 10^4$ and 4.74 s^{-1} are evaluated by a fit to single-exponential function.

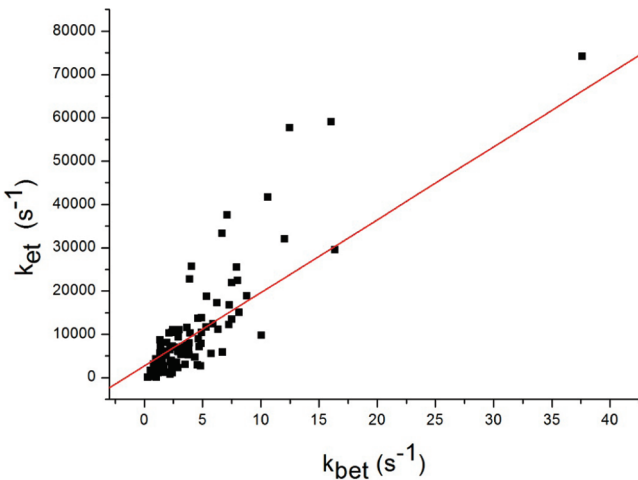


Figure 10. Linear correlation between photoinduced electron transfer and back electron transfer rate constant.

When the TiO_2 thick film is substituted, the measurements of excited-state lifetimes and fluorescence trajectories are conducted successively up to 100 dye molecules adsorbed. The resulting IFET and back ET rate constants are analogously analyzed to yield $(1.0 \pm 0.6) \times 10^4$ and $6.3 \pm 1.6 \text{ s}^{-1}$, respectively, while the

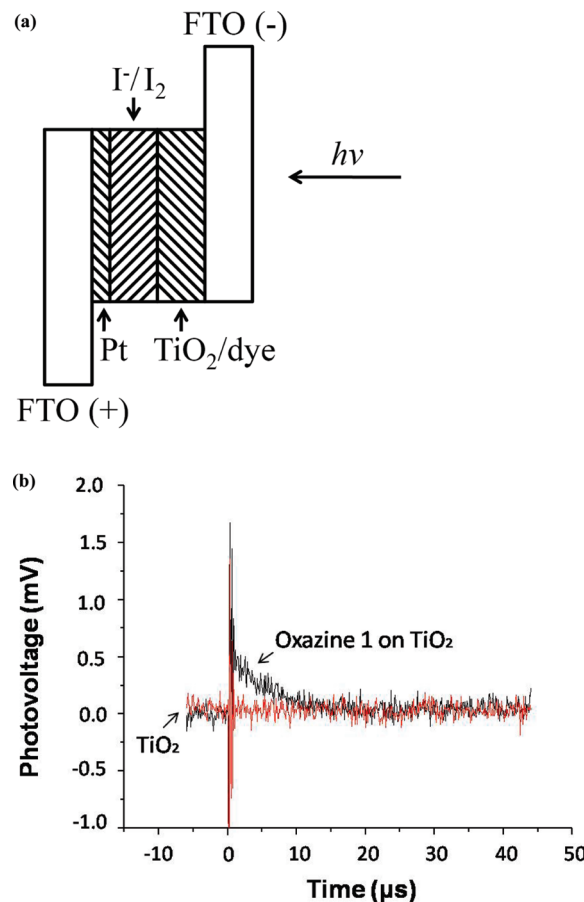


Figure 11. (a) Schematic of a dye-sensitized solar cell device. (b) Plot of photovoltage response vs time acquired from the dye-sensitized solar cell device, which was excited with a pulsed laser at 630 nm. A photovoltage decay was obtained when the device comprised oxazine 1 dye, but it reduced to zero when the dye was removed.

average lifetime is $2.7 \pm 0.3 \text{ ns}$. These results are consistent with those determined with a TiO_2 thin film. Given a constant TiO_2 NPs size, the way to prepare for the solid film does not lead to a significant difference for determining these kinetic parameters.

The process of photoinduced ET involves charge ejection from the oxazine 1 lowest unoccupied molecular orbital (LUMO $\sim 2.38 \text{ eV}$) into a large energetically accessible density of states within the conduction band of the TiO_2 ($\sim 4.4 \text{ eV}$), while the back ET involves thermal relaxation of electrons from the conduction band or from a local trap (energetically discrete states) back to the singly occupied molecular orbital (SOMO) of the oxazine 1 cation.³⁵ It is interesting to find a linear correlation with a slope of 1.7×10^3 between IFET and back ET rate constants, as shown in Figure 10. Despite differences in the mechanisms, k_{bet} increases almost in proportion to k_{et} in this work. Such a strong correlation between forward and backward ET rate constants suggests that for different molecules of oxazine 1 the energetics for electron transfer remains the same but the electronic coupling between the excited state of the dye molecules and the conduction band of the solid film varies widely.⁴² Both forward and backward ET processes are affected similarly by geometric distance and orientation between electron donor and acceptor.

C. Photovoltage Response in DSSC. When the oxazine 1 dye-sensitized solar cell is assembled (Figure 11a), as described in the Experimental Section, and excited with a 10 Hz, 5–8 ns pulsed laser at 630 nm, an appreciable photovoltage response can be measured. When the dye sensitizer is removed from the solar cell,

the photovoltage becomes zero. As shown in Figure 11b, the photovoltage decay for the ensemble-averaged experiment is on the order of 10^{-5} s, which is about 1 order of magnitude faster than the average IFET rate determined in the single molecule experiments. The discrepancy might arise from at least two factors. First, as mentioned above, some excited dye molecules undergoing very efficient IFET process are quenched before they can fluoresce for detection. If these molecules are taken into account, then the average IFET rate constant should become larger. Second, the complicated factors associated with a solar cell device might cause the deviation. The photovoltage response is an outcome associated with several factors such as competition between forward ET rate and recombination rate of oxidized dye molecules with electrons from different sources, concentration of dye molecules, electrolyte species, and concentration and pH regulation. Some factors might enhance the forward ET but slow the backward ET, such that the ensemble-averaged experiment gives a faster photovoltage response. Unlike this case, cyanine and xanthene dyes deposited on In_2O_3 and SnO_2 electrodes show very efficient electron transfer.^{55–57} The quantum yield for sensitized electron current depends mainly on competition between forward electron transfer and recombination processes of the oxidized dye and electrons. Single molecule measurements can unveil the detailed photoinduced ET behavior of individual molecules adsorbed on solid film without suffering from interference by those factors inherent in the ensemble-averaged experiments. The results also help justify the influence of these complicated factors in making a solar cell device.

V. Conclusion

A photosensitized interfacial electron transfer on oxazine 1- TiO_2 NPs system has been investigated at a single molecule

level. The fluorescence lifetimes determined among different single dye molecules are widely spread, because of microenvironmental influence. These lifetimes are in proximity to those measured on the bare coverslip, indicative of the IFET inefficiency for those dye molecules sampled in this work. However, some molecules may proceed via a very efficient IFET process but fail to be detected. Due to a shorter triplet excursion, a three-level energy model can be validly applied to determine the IFET kinetics of the single dye molecules on the TiO_2 NPs surface based on the fluorescence trajectories. The efficacy of IFET thus obtained agrees with that determined by the fluorescence lifetime method. The IFET processes are found to be inhomogeneous, with a rate constant varying from molecule to molecule. The reactivity and rate of ET fluctuation of the same single molecule are the main source resulting in fluorescence intensity fluctuation. These phenomena, which are obscured in the ensemble-averaged system, are attributed to microenvironment variation for each single molecule. The oxazine 1 dye is apparently unsuitable for application to the DSSC design, because of its lower ET rates. Nevertheless, the single molecule spectroscopy provides a potential tool looking into the microscopic ET behaviors for different dye molecules to facilitate the working efficiency for the cell design. In addition, it is capable of detecting a low ET quantum yield, which is difficult to measure with conventional ensemble-averaged methods.

Acknowledgment. The authors wish to thank Prof. Kuochuan Ho and Dr. Ying-Chan Hsu for helping with the techniques to synthesize the TiO_2 nanoparticles film and to form the DSSC device. This work is supported by National Science Council, Taiwan, Republic of China under contract no. NSC 96-2113-M-002-027.